# Characteristics of electro-refractive modulating based on Graphene-Oxide-Silicon waveguide

**Chao Xu, Yichang Jin, Longzhi Yang, Jianyi Yang, and Xiaoqing Jiang***

*Department of Information science and Electronics Engineering, Zhejiang University, Hangzhou, 310027, China*
*iseejxq@zju.edu.cn*

**Abstract:** Graphene has attracted a high level of research interest because of its outstanding electronic transport properties and optical properties. Based on the Kubo formalism and the Maxwell equations, it's demonstrated that the optical conductivity of graphene can be controlled through the applied voltage. And we find that the graphene-oxide-silicon (GOS) based waveguide can be made into either the electro-absorptive or electron-refractive modulators. Using graphene as the active medium, we present a new electro-refractive Mach-Zender interferometer based on the GOS structure. This new GOS-based electron-refractive modulation mechanism can enable novel architectures for on-chip optical communications.



**OCIS codes:** (130.3120) Integrated Optics devices; (230.7370) Waveguides; (250.7360) Waveguide modulators.

## References and links

1. G. T. Reed, G. Mashanovich, F. Y. Gardes, and D. J. Thomson, "Silicon optical modulators," Nat. Photonics **4**(8), 518–526 (2010).
2. R. A. Soref and B. R. Bennett, "Electrooptical effects in silicon," IEEE J. Quantum Electron. **23**(1), 123–129 (1987).
3. L. Alloatti, D. Korn, R. Palmer, D. Hillerkuss, J. Li, A. Barklund, R. Dinu, J. Wieland, M. Fournier, J. Fedeli, H. Yu, W. Bogaerts, P. Dumon, R. Baets, C. Koos, W. Freude, and J. Leuthold, "42.7 Gbit/s electro-optic modulator in silicon technology," Opt. Express **19**(12), 11841–11851 (2011).
4. A. Liu, R. Jones, L. Liao, D. Samara-Rubio, D. Rubin, O. Cohen, R. Nicolaescu, and M. Paniccia, "A high-speed silicon optical modulator based on a metal-oxide-semiconductor capacitor," Nature **427**(6975), 615–618 (2004).
5. Q. Xu, B. Schmidt, S. Pradhan, and M. Lipson, "Micrometre-scale silicon electro-optic modulator," Nature **435**(7040), 325–327 (2005).
6. S. Y. Zhu, G. Q. Lo, and D. L. Kwong, "Components for silicon plasmonic nanocircuits based on horizontal Cu-$SiO_2$-Si-$SiO_2$-Cu nanoplasmonic waveguides," Opt. Express **20**(6), 5867–5881 (2012).
7. A. K. Geim and K. S. Novoselov, "The rise of graphene," Nat. Mater. **6**(3), 183–191 (2007).
8. T. Gu, N. Petrone, J. F. McMillan, A. V. D. Zande, M. Yu, G. Q. Lo, D. L. Kwong, J. Hone, and C. W. Wong, "Regenerative oscillation and four-wave mixing in graphene optoelectronics," Nat. Photonics **6**(8), 554–559 (2012).
9. K. Kim, J. Y. Choi, T. Kim, S. H. Cho, and H. J. Chung, "A role for graphene in silicon-based semiconductor devices," Nature **479**(7373), 338–344 (2011).
10. M. Liu, X. Yin, E. Ulin-Avila, B. Geng, T. Zentgraf, L. Ju, F. Wang, and X. Zhang, "A graphene-based broadband optical modulator," Nature **474**(7349), 64–67 (2011).
11. H. Li, Y. Anugrah, S. J. Koester, and M. Li, "Optical absorption in graphene integrated on silicon waveguides," arXiv: 1205.4050v1, 2012.
12. S. J. Koester and M. Li, "High-speed waveguide-coupled graphene-on-graphene optical modulators," Appl. Phys. Lett. **100**(17), 171107 (2012).
13. M. Liu, X. Yin, and X. Zhang, "Double-layer graphene optical modulator," Nano Lett. **12**(3), 1482–1485 (2012).
14. J. Christensen, A. Manjavacas, S. Thongrattanasiri, F. H. L. Koppens, and F. J. de Abajo, "Graphene Plasmon Waveguiding and Hybridization in Individual and Paired Nanoribbons," ACS Nano **6**(1), 431–440 (2012).
15. G. W. Hanson, "Quasi-transverse electromagnetic modes supported by a graphene parallel-plate waveguide," J. Appl. Phys. **104**(8), 084314 (2008).
16. Q. Bao, H. Zhang, B. Wang, Z. Ni, C. Haley, Y. Xuan, Y. Wang, C. H. Y. X. Lim, D. Y. Tang, and K. P. Loh, "Broadband graphene polarizer," Nat. Photonics **5**(7), 411–415 (2011).
17. G. W. Hanson, "Dyadic Green's functions and guided surface waves for a surface conductivity model of graphene," J. Appl. Phys. **103**(6), 064302 (2008).

#172611 - $15.00 USD Received 16 Jul 2012; revised 23 Aug 2012; accepted 7 Sep 2012; published 17 Sep 2012

18. V. P. Gusynin, S. G. Sharapov, and J. P. Carbotte, "Magneto-optical conductivity in graphene," J. Phys. Condens. Matter **19**(2), 026222 (2007).
19. F. Wang, Y. Zhang, C. Tian, C. Girit, A. Zettl, M. Crommie, and Y. R. Shen, "Gate-variable optical transitions in graphene," Science **320**(5873), 206–209 (2008).
20. L. Ren, Q. Zhang, J. Yao, Z. Sun, R. Kaneko, Z. Yan, S. Nanot, Z. Jin, I. Kawayama, M. Tonouchi, J. M. Tour, and J. Kono, "Terahertz and Infrared Spectroscopy of Gated Large-Area Graphene," Nano Lett. **12**(7), 3711–3715 (2012).
21. J. Yan, Y. Zhang, P. Kim, and A. Pinczuk, "Electric Field Effect Tuning of Electron-Phonon Coupling in Graphene," Phys. Rev. Lett. **98**(16), 166802 (2007).
22. X. L. Wen and Y. L. Long, "An implementation of a root-finding algorithm for transcendental functions in a complex plane," J. Numer. Methods & Comput. Appl. No. **2**, 88–92 (1994).
23. K. I. Bolotin, K. J. Sikes, Z. Jiang, M. Klima, G. Fudenberg, J. Hone, P. Kim, and H. L. Stormer, "Ultrahigh electron mobility in suspended graphene," Solid State Commun. **146**(9-10), 351–355 (2008).

## Introduction

The electro-optic modulator is one of the most important optoelectronic devices, which is used to modulate a light beam propagating either in free space or in an optical waveguide. In addition, these modulators can be classified as either electro-refractive or electro-absorptive type. It is well known that by applying an electric field to a material, its real and imaginary refractive indices could be changed. The change in the real part of the refractive index ( $\Delta n$ ) is defined as electro-refraction, whereas the change in the imaginary part of the refractive index ( $\Delta\alpha$ ) is known as electro-absorption [1]. So far, the proposed silicon modulators, which are electro-refraction, are mostly based on the free-carrier dispersion effect in silicon [2].

However, the electro-optic properties of the silicon are usually poor so that a conventional silicon modulator has a very large footprint [3,4]. Although micro-ring silicon modulator can significantly reduce the footprint, but it also decreases the operation bandwidth and thermal stability [5]. Nanoplasmonics paves the way to scale down the dimension of optical devices, and several plasmonic modulators have been proposed. The"PlasMOStor" presented by Dionne *et al.* [6] is very compact, but due to the surface plasmon polaritons (spps), it has inherently large loss and limits the operation speed. Recent research on graphene has shown the potential to deal all these challenges.

Graphene, a two-dimensional version of graphite, consisting of carbon atoms arranged in a hexagonal lattice, has attracted a great deal of interest. Intrinsic graphene is a zero band-gap semiconductor which is very suitable for nano-electronic applications [7,8]. And its transport characteristics and conductivity can be tuned conveniently by electrostatics, leading to the possibility of modulator [9]. The waveguide-integrated graphene based electro-absorption modulator was first reported by Liu [10]. This graphene-based electro-absorption optical modulation mechanism, with combined advantages of compact footprint, low operation voltage and ultrafast modulation speed across a broad range of wavelengths, can enable novel architectures for on chip optical communications. So far all of these graphene based optical modulators are the electro-absorptive [10–13]. The absorption directly modulates the intensity of a propagating mode. And in these modulators, the graphene interband absorption plays a key role [10,13].

In this paper, we analyze the electro-refractive modulating mechanism based on graphene-oxide-silicon structure. The optical conductivity of graphene is calculated by the Kubo formalism at $T$ = 300 K, both interband and intraband absorption are considered. The refractive index change caused by the variation of the graphene conductivity can be used to shift the relative phase of two propagating waves so that they interfere either constructively or destructively, thus realizing the transition between on- and off- resonance states. A GOS-based MZI is presented to demonstrate the new electro-refractive modulating mechanism.

#172611 - $15.00 USD Received 16 Jul 2012; revised 23 Aug 2012; accepted 7 Sep 2012; published 17 Sep 2012

**Model of the GOS structure**

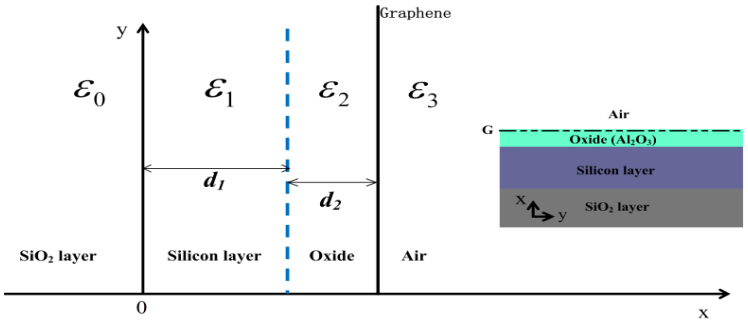


Fig. 1. 2D model in which graphene is considered as a conductive interface between Oxide ($Al_2O_3$) and air. During the calculation, the oxide is defined as $Al_2O_3$.$\varepsilon_0 = 1.455^2$,$\varepsilon_1 = 3.455^2$,$\varepsilon_2 = 1.746^2$,$\varepsilon_3 = 1$. Inset is the cross-section of the GOS waveguide. G represents graphene in the inset figure.

The electromagnetic responses of graphene-oxide-silicon are numerically stimulated based on the model in Fig. 1. The wave propagates in the Z-direction. Based on the classical electromagnetic description, we could get the Maxwell equation as follows,

$$\nabla \times H = \varepsilon \varepsilon_r \frac{\partial E}{\partial t} + \sigma E \tag{1}$$

$$\nabla \times \mathrm{E} = -\mu \frac{\partial H}{\partial t} \tag{2}$$

All units are in SI system, and the time variation is $e^{j\omega t}$. Considering the time oscillation, for the transverse magnetic mode, the Eq. (1) and (2) can be written as follows, $\varepsilon_i$ is the relative permittivity of region *i*,

$$\left( \frac{\partial^2}{\partial x^2} + \frac{\partial^2}{\partial z^2} + \varepsilon_i k_0^2 \right) H_y(x,z) = 0 \tag{3}$$

As Fig. 1 shows, the 2D waveguide can be treated as a four-layer planar waveguide. It is noted that graphene is modeled as a thin layer with thickness of $t_g = 0.35$ nm between the oxide layer and the air cladding. This value of $t_g$ can be reasonably well converged with respect to the $t_g \to 0$ limit [14]. That is to say this thin conducting graphene layer can be represented by an infinitesimally thin, local two-sided surface. In our model, there are three asymmetric interfaces, the silica/silicon interface, the silicon/oxide interface and the graphene/oxide interface. In this case, we only consider the surface conductivity of graphene because the others are all dielectric layers, and the boundary condition for this structure can be rewritten as this,

$$\begin{aligned} &\hat{n} \times (E_+ - E_-) = 0 \\ &\hat{n} \times (H_+ - H_-) = \sigma E \\ &\lim_{x \to \pm\infty} E, H = 0 \end{aligned} \tag{4}$$

At graphene/oxide interface, $\sigma$ is the conductivity of graphene, while at the other two interfaces, $\sigma = 0$ [15,16]. For TM polarization, after establishing coordinate, and matching the boundary condition, we can get the eigen-equation like this:

#172611 - $15.00 USD Received 16 Jul 2012; revised 23 Aug 2012; accepted 7 Sep 2012; published 17 Sep 2012

$$\begin{aligned}
&\arctan(T_2 Q_3) + \arctan(T_1) + m\pi = \gamma_1 d_1 \\
&Q_3 = -\frac{1 - R\tanh(\gamma_2 d_2)}{R - \tanh(\gamma_2 d_2)} \\
&R = \frac{\varepsilon_3 \gamma_2}{\varepsilon_2 \gamma_3}\left(\frac{\sigma\gamma_3}{j\omega\varepsilon_3\varepsilon} - 1\right)
\end{aligned} \tag{5}$$

where $m$ is the mode order, $T_1 = \varepsilon_1\gamma_0/\varepsilon_0\gamma_1$ , $T_2 = \varepsilon_1\gamma_2/\varepsilon_2\gamma_1$ , $T_3 = \varepsilon_1\gamma_3/\varepsilon_3\gamma_1$ , $\gamma_1^2 = k_0^2\varepsilon_1 - \beta^2$ , $\gamma_i^2 = \beta^2 - k_0^2\varepsilon_i\,(i = 0,2,3)$, $k_0 = \omega\sqrt{\mu\varepsilon}$.

*Optical conductivity of Graphene*

The dynamic optical conductivity of graphene can be determined from the Kubo formalisms [17,18], consisting of intraband and interband contributions,

$$\begin{aligned}
\sigma(\omega,\mu_c,\tau,T) = \frac{je^2(\omega - j\tau^{-1})}{\pi\hbar^2}\Bigg[&\frac{1}{(\omega - j\tau^{-1})^2}\int_0^\infty \xi\left(\frac{\partial f_d(\xi)}{\partial\xi} - \frac{\partial f_d(-\xi)}{\partial\xi}\right)d\xi \\
&-\int_0^\infty \frac{f_d(-\xi) - f_d(\xi)}{(\omega - j\tau^{-1})^2 - 4(\xi/\hbar)^2}\,d\xi\Bigg]
\end{aligned} \tag{6}$$

where $e$ is the charge of an electron, $\xi$ is the energy, $\hbar$ is the reduced Planck's constant, $f_d(\xi) = \left(e^{(\xi-\mu_c)/k_BT} + 1\right)^{-1}$ is the Fermi-Dirac distribution, $\omega$ is the radian frequency, $k_B$ is the Boltzmann's constant, $T$ is the temperature, $\mu_c$ is the chemical potential, which can be varied by doping and/or an applied bias, $\tau$ is the relaxation time ($\tau^{-1}$ is the scattering rate), $j$ is the imaginary unit and $e^{j\omega t}$ is the time variation. The first part in Eq. (6) is due to the intraband contribution and the second is due to interband contribution. The intraband contribution can be derived and simplified as,

$$\sigma_{\mathrm{int}ra}(\omega) = -j\frac{e^2 k_B T}{\pi\hbar^2(\omega - j\tau^{-1})}\left[\frac{\mu_c}{k_B T} + 2\ln\left(e^{-\mu_c/k_BT} + 1\right)\right] \tag{7}$$

while the interband can be approximated as, for $k_BT << |\mu_c|, \hbar\omega$:

$$\sigma_{\mathrm{int}er}(\omega) = \frac{-je^2}{4\pi\hbar}\ln\left(\frac{2|\mu_c| - (\omega - j\tau^{-1})\hbar}{2|\mu_c| + (\omega - j\tau^{-1})\hbar}\right) \tag{8}$$

Based on the Kubo formalisms, we calculated the graphene's conductivity at $T$ = 300 $K$, $\lambda$=1550 nm . The conductivity is normalized by $\sigma_0 = \pi e^2/2h = 6.085\times10^{-5}$ S . Figure 2 shows how the intraband absorption and interband absorption contribute to the graphene conductivity, respectively. In this way, the Kubo formalism provides the necessary conductivity $\sigma = \sigma_r + j\sigma_i$ . From Fig. 2(b), we can see that the imaginary part of graphene conductivity has a peak value. Obviously, it was caused by the interband absorption for that the Eq. (8) is a non-monotonic function, an abrupt change in $\sigma_{\mathrm{inter}}$ when $2|\mu_c| = \omega\hbar$ , which in this case $\mu_c \approx 0.4$ eV . The trace of critical drive voltage for graphene's chemical potential can be defined as [19–21]:

$$|\mu_c| \approx \left|E_F(V_g)\right| = \hbar v_F\sqrt{\pi\left|a_0(V_g - V_{Dirac})\right|} \tag{9}$$

#172611 - $15.00 USD Received 16 Jul 2012; revised 23 Aug 2012; accepted 7 Sep 2012; published 17 Sep 2012

where $V_{Dirac}$=0.8 V , is the voltage offset caused by natural doping, $\upsilon_F$=0.9×10$^6$ m/s , is the Fermi velocity of Dirac fermions in Graphene,and $a_0 \approx 9\times10^{16}$ m$^{-2}$V$^{-1}$ estimated from a single capacitor model [10]. For Simplicity, $\left|V_g - V_{Dirac}\right|$ would be considered as the applied voltage. Thus, the conductivity of graphene can be dynamically tuned by the applied voltage.

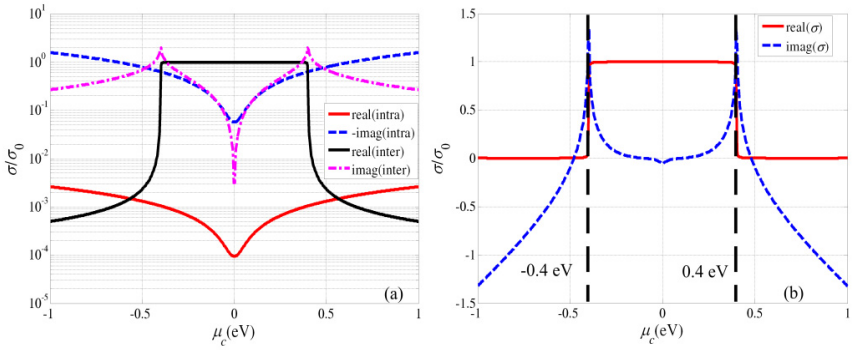


Fig. 2. Interband and intraband conductivity (unit of S) as a function of chemical potential at wavelength 1550 nm,$T = 300\ K, \tau = 5 \times 10^{-13}$ s.

In this GOS-based structure, the complex conductivity of graphene make the root of the eigen-value equation be complex. It's really hard to find the roots of the transcendental equation in complex plane. Here we use a semi-analytical method to calculate the propagation constants in complex plane by Cauchy contour integration (CCI) [22].

**Characteristics and discussion**

The following results are for the TM fundamental mode ($m = 0$ in Eq. (5)) of a four-layer planar waveguide based on graphene-oxide-silicon structure, as illustrated schematically in Fig. 1. For simplicity, the device structure consists of a graphene monolayer attached to the oxide layer ($Al_2O_3$) grown on a silicon layer with a silica layer.

Assuming the thickness of the oxide layer ($d_2$ = 10 nm),without graphene layer (which means $\sigma = 0$ in calculation),we can get the TM mode as shown in Fig. 3. We can see that from Fig. 3 as $d_2$ decreases, the effective index and the loss decreases too. And the electrical field in oxide layer is larger than that in silicon. Apparently, though the oxide layer is much thinner than the silicon layer, the TM mode is still disturbed.

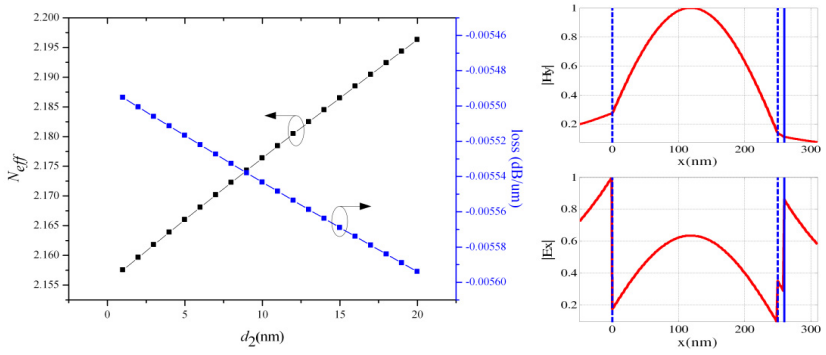


Fig. 3. the effective index of the TM mode varies with $d_2$ (the thickness of the oxide layer), the left inset is the mode distribution of Hy and Ex when $d_1$ = 250 nm, $d_2$ = 10 nm.

#172611 - $15.00 USD Received 16 Jul 2012; revised 23 Aug 2012; accepted 7 Sep 2012; published 17 Sep 2012

By applying a bias voltage on this GOS structure waveguide, the chemical potential of graphene would be changed; the charge-carrier density in graphene changes and the modulation can be realized. Once the structure (shown in Fig. 1) is applied with voltage, the effective index of the TM mode would be changed. From Fig. 4, we can see that as the applied voltage increase, $\mu_c$ would increase continuously. However, $N_{eff}$ (the effective index of the TM mode) would first increase and then decrease, which shares the same trend of variability with the imaginary of the graphene optical conductivity as shown in Fig. 2. And the value of $N_{eff}$ would reach its maximum value when $\mu_c \approx 0.4\,\mathrm{eV}$. Compared with the carrier dispersion effect, the variation of $N_{eff}$ is much larger, which shows the potential possibility to be made into electro-refractive modulator. If the work domain is settled between 0 eV and 0.4 eV (the applied voltage is about 1.6 V when $\mu_c \approx 0.4\,\mathrm{eV}$), as shown in Fig. 4, we can see that the electro-absorption is the best option, which was reported in [10]. However, as the $\mu_c$ increases with the voltage, the loss would decrease, and that is benefit for an electro-refraction. Based on these theoretical analyses, we design a novel GOS-based MZI.

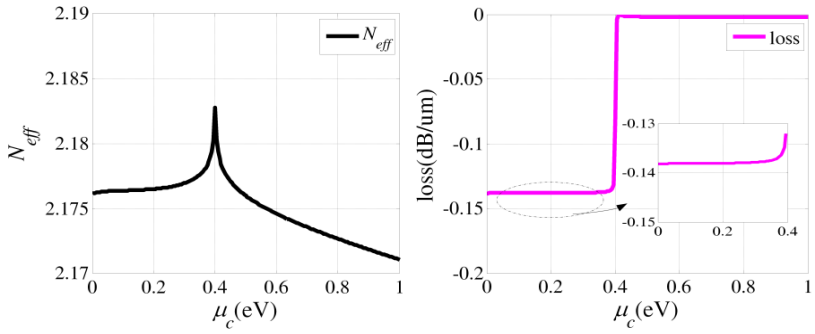


Fig. 4. the effective index and the loss of the TM mode varies with $\mu_c$ (the chemical potential of graphene) when $d_1$ = 250 nm, $d_2$ = 10 nm.

*GOS-based Mach-Zehnder interferometers*

MZI is a basic building block for many optical devices. As we have proved in previous sections, the graphene-oxide-silicon waveguide can obtain large variation of the effective index. We propose the integration of a MZI implemented with the graphene-oxide-silicon structure shown in Fig. 5. The two arms of the MZI consist of the graphene-oxide-silicon waveguide, which would be applied with voltage to modulate the light transmission. The Fig. 5(c) is the cross section of the MZI-arm. The thickness of the silicon layer and the oxide layer is 250 nm, 10 nm, respectively. The silicon layer is shallowly doped. Similar to the structure shown in [10], a gold electrode is extended towards the waveguide by depositing a platinum film on top of the graphene layer, and the other gold electrode is deposited on the $P^+$ doped region. And the minimum distance between platinum and waveguide should be controlled at 500 nm to avoid the effect on the optical mode, which is reported in [10].

#172611 - $15.00 USD Received 16 Jul 2012; revised 23 Aug 2012; accepted 7 Sep 2012; published 17 Sep 2012

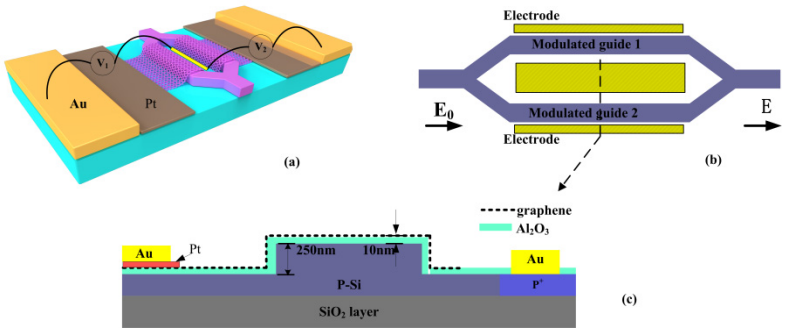


Fig. 5. The sketch map of the GOS based MZI. (a) is the schematic 3D drawing of the MZI. (b) is the vertical show of the MZI. (c) is the cross section of the MZI-arm;

According to the interference theory of the MZI, the normalized transmission, $T(\lambda)$, can be expressed as follows:

$$T(\lambda)=\frac{1}{4}\times\left[\exp(-\alpha_0 L)+\exp(-\alpha_1 L)+2\exp(-\frac{\alpha_0 L+\alpha_1 L}{2})\cos(\Delta\phi)\right] \qquad (10)$$

where $\Delta\phi=2\pi/\lambda\,\Delta N_{eff}L$, $\alpha_0$, $\alpha_1$ is the propagation loss of the two arms, respectively, $L$ is the length of the MZI-arm. To avoid the large loss, the guide 1 is modulated at 0.4 eV (the applied voltage is about 1.6 V), and the guide 2 is modulated in the region $\mu_c > 0.4\,\text{eV}$. Figure 6 shows the normalized output power as a function of $\mu_c$ variation in guide 2. In this case, the lengths of the arms are 200 μm. Thus, we can realize the new electro-refractive MZI modulator. Different from the traditional silicon MZI, this modulator does not need the carrier dispersion effect. And because the carrier mobility of the suspended graphene exceed 200,000 $cm^2V^{-1}s^{-1}$ at room temperature [23], this new MZI may have ultra high operating speed, depending on the carrier density and graphene quality.

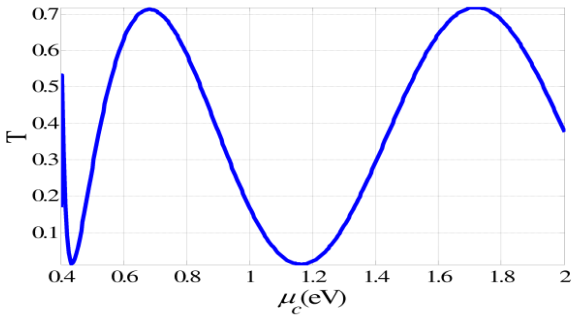


Fig. 6. The transmission of the GOS MZI varies with the chemical potential.

## Conclusions

With the Kubo formalism and the Maxwell equations, we proved that the graphene layer would influence the optical mode in the silicon waveguide and it can be used as the active medium to modulate light transmission. By applying the voltage to the graphene-oxide-silicon waveguide, the real and imaginary refractive indices have very great variation. This new effect, which is decided by the chemical potential of the graphene, offers a mean for electrically controlled optical modulation in a GOS waveguide either in electro-refractive or electro-absorptive style. Compared with the electro-absorptive modulator, the electro-refractive is more convenient to

#172611 - $15.00 USD Received 16 Jul 2012; revised 23 Aug 2012; accepted 7 Sep 2012; published 17 Sep 2012

control, and the interference mechanism can achieve better extinction ratio. Thus, we also proposed a novel GOS-based MZI with the advantage of potential high operating speed.

**Acknowledgment**

This work is supported by the Natural Science Foundation of China (No. 6177055).

#172611 - $15.00 USD Received 16 Jul 2012; revised 23 Aug 2012; accepted 7 Sep 2012; published 17 Sep 2012